Loops & Legs 2022, Ettal, Germany 26 April 2022

ZH Production in Gluon Fusion @ 2-loops

Stephen Jones
IPPP, Durham / Royal Society URF

In collaboration with:
Chen, Davies, Heinrich, Kerner, Klappert,
Mishima, Schlenk, Steinhauser

[2204.05225 + 2011.12325]

Durham University

THE ROYAL SOCIETY

Outline

Motivation & Background

Setup of Calculation

- Tensor decomposition/ diagram generation/ γ_5 / Reduction
- Numerically evaluating amplitudes with pySecDec

Results, Comparisons and Open Issues

Overview of $pp \to ZH$ (I)

Consider the matrix element for $pp \to ZH$ with QCD corrections

Various channels contribute: $q\bar{q} \to ZH$ and $gg \to ZH$

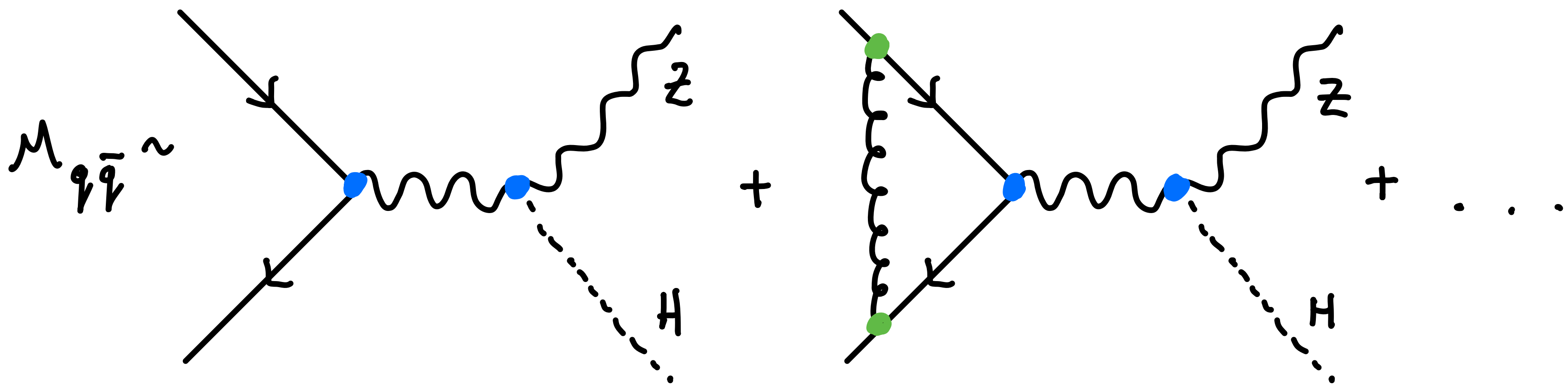

The $gg \to ZH$ channel is **loop-induced** (i.e. LO in this channel is 1-loop)

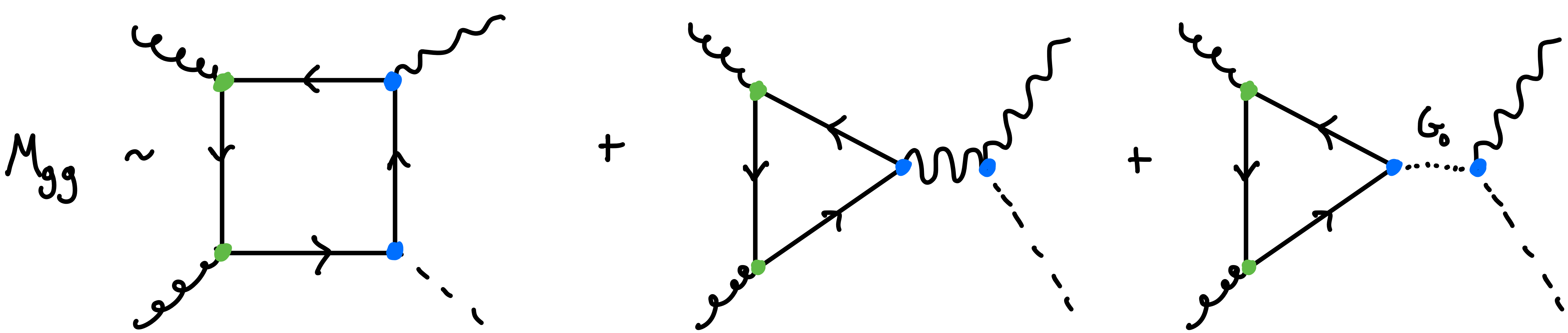

Overview of $pp \to ZH$ (II)

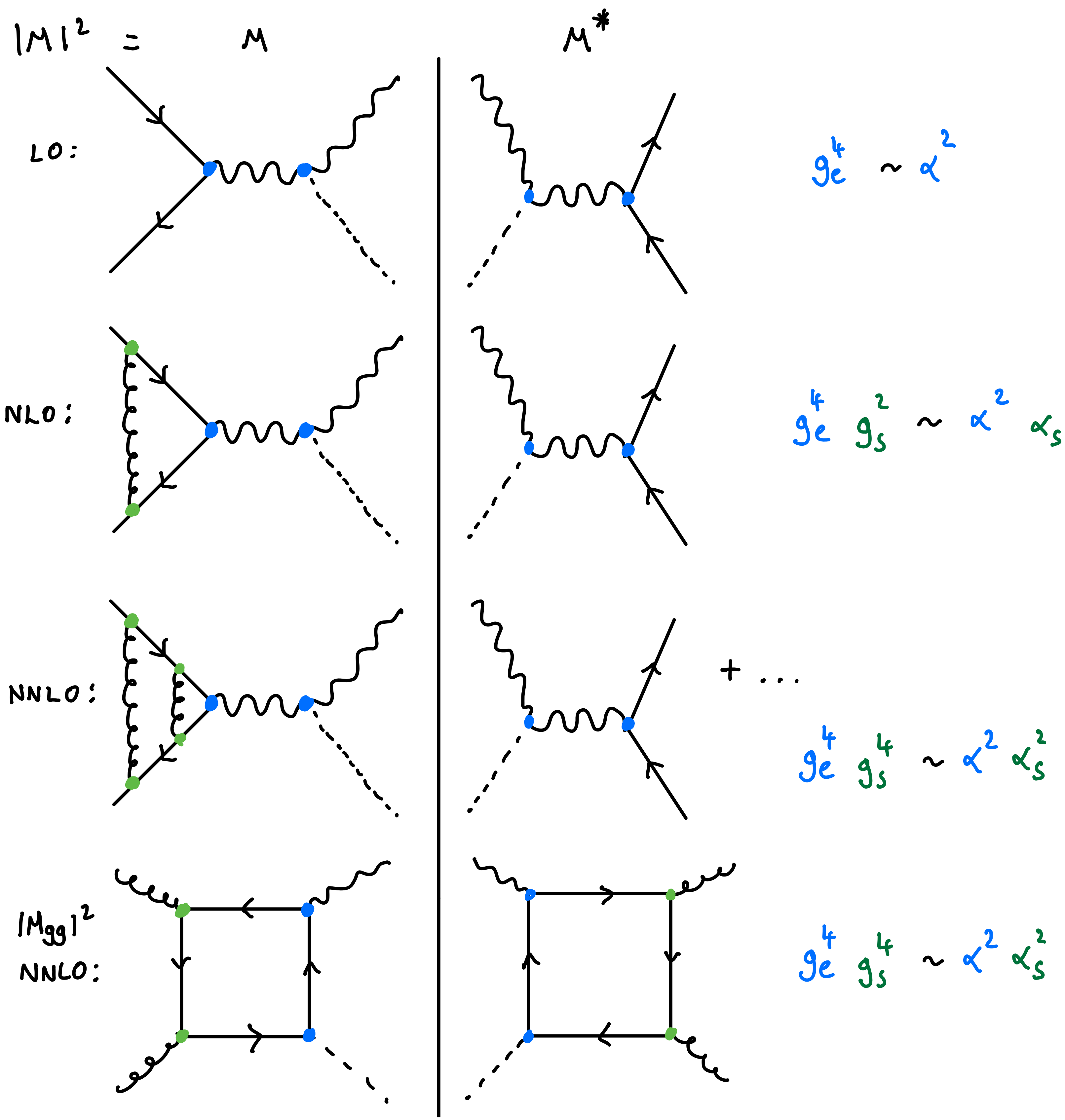

The $gg \to ZH$ channel contributes to $pp \to ZH$ starting at NNLO in QCD

However due the large gluon-gluon luminosity at the LHC it contributes significantly (~10%) to the total cross section

Overview of $pp \to ZH$ (III)

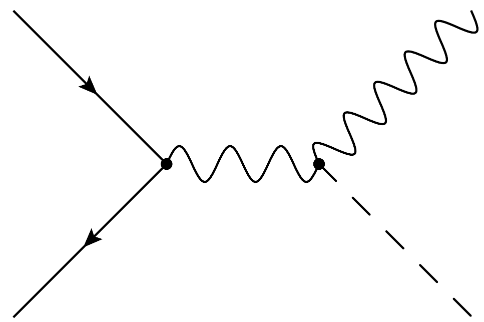

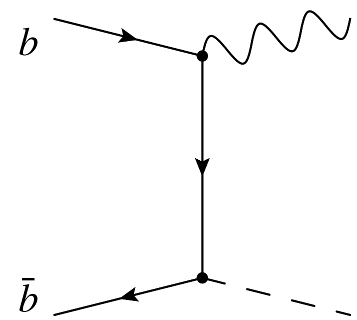

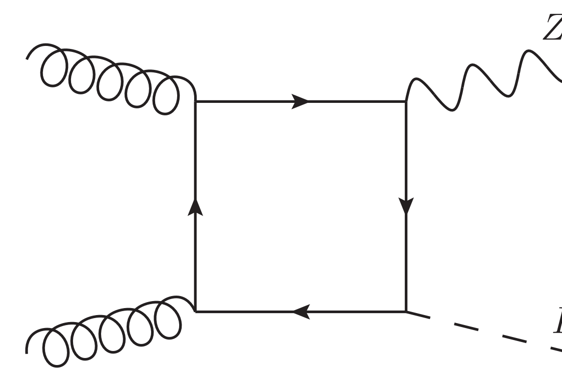

Drell-Yan piece (NNLO known)

Brein, Djouadi, Harlander 03;
Ferrera, Grazzini, Tramontano 14;
See also: Kumara, Mandal, Ravindran 14

$b\bar{b}$ piece (NNLO known)

Ahmed, Ajjath, Chen, Dhani, Mukherjee, Ravindran 19

Gluon-fusion piece
~10% of total xs.
~100% scale unc.

+ $q\bar{q}$ piece with closed top loops (1-3%)

Available in various codes:

HAWK (NLO QCD + NLO EW)

Denner, Dittmaier, Kallweit, Mück 14

vh@nnlo (NNLO QCD + NLO EW)

Harlander, Klappert, Liebler, Simon 18;
Brein, Harlander, Zirke 12

MCFM (NNLO QCD)

Campbell, Ellis, Williams 16

GENEVA (NNLL′+NNLO with PS)

Alioli, Broggio, Kallweit, Lim, Rottoli 19

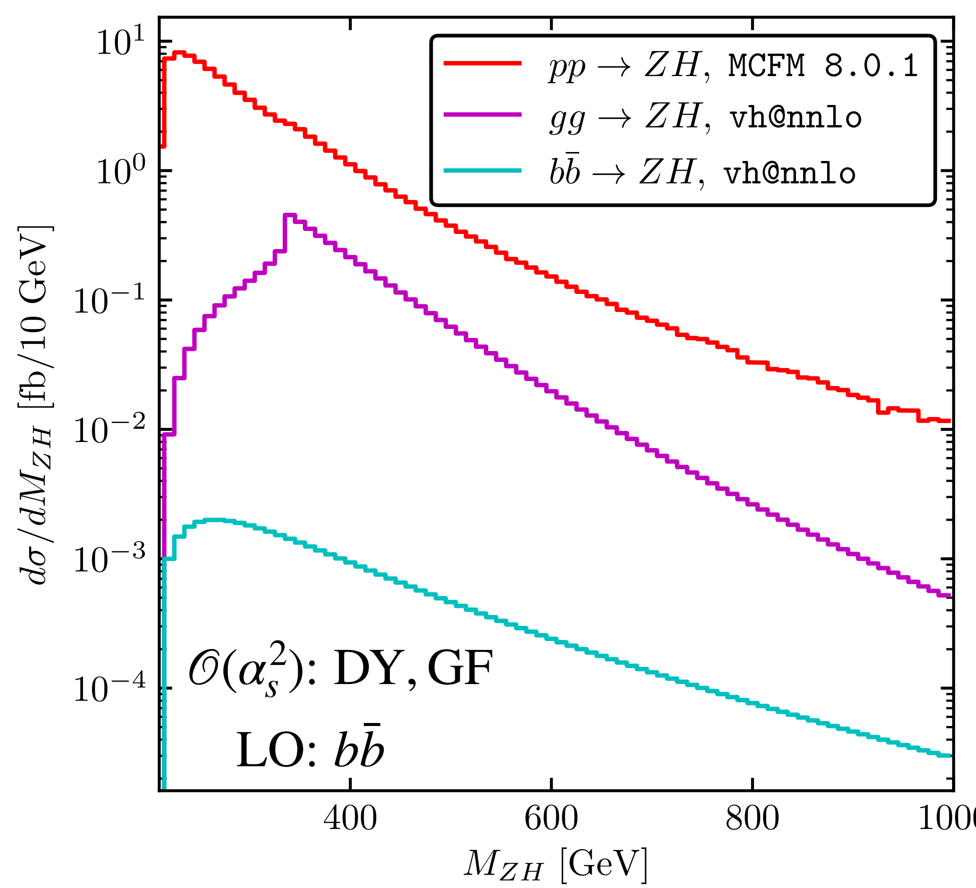

Harlander, Klappert, Liebler, Simon 18

ZH in Gluon Fusion

Full leading order (loop induced)
Dicus, Kao 88; Kniehl 90

NLO in the limit of $m_t \to \infty$ $(K \approx 2)$
Altenkamp, Dittmaier, Harlander, H. Rzehak, Zirke 12

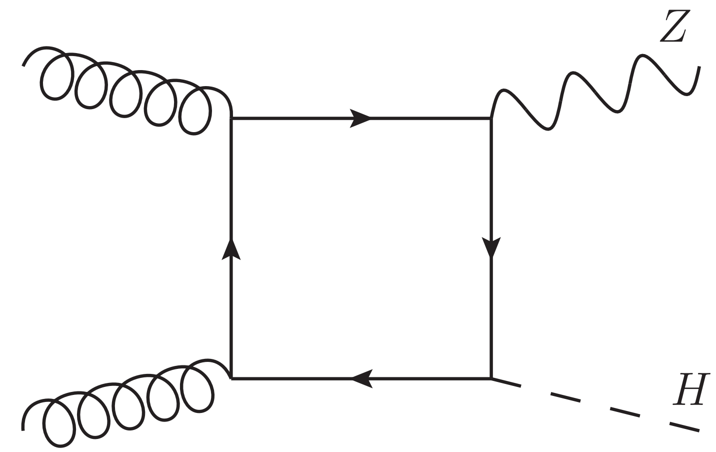

Virtual Corrections:

$1/m_t^8$ Expansion + Padé approx
Hasselhuhn, Luthe, Steinhauser 17

$1/m_t^{10}$ & m_t^{32} Expansion + Padé approx
Davies, Mishima, Steinhauser 20

Full numerical result
Chen, Heinrich, SPJ, Kerner, Klappert, Schlenk 20

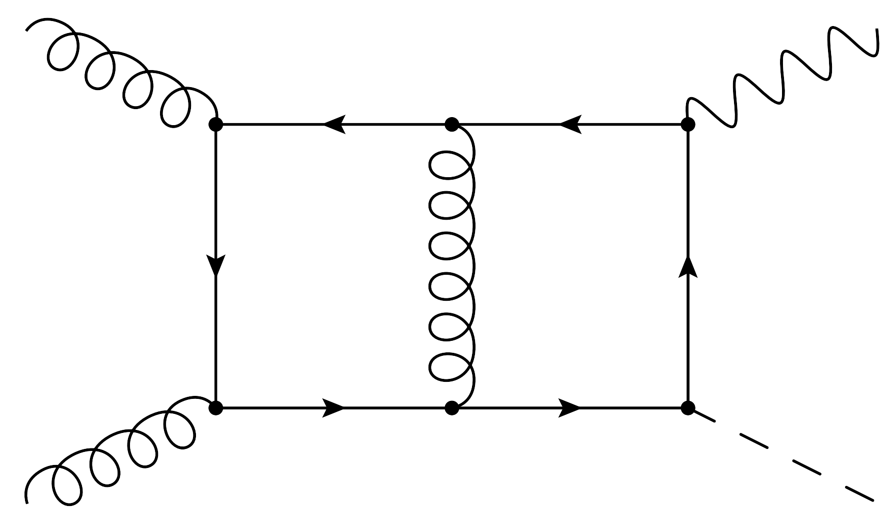

p_T^4 Expansion
Alasfar, Degrassi, Giardino, Gröber, Vitti 21

$p_T^4 + m_t^{12}$ Expansion + Padé approx
Bellafronte, Degrassi, Giardino, Gröber, Vitti 22

NLO result: small m_z, m_h Expansion
Wang, Xu, Xu, Yang 21

Setup & Amplitudes

Diagrams: $gg \to ZH$

Leading Order (1-loop) Diagrams

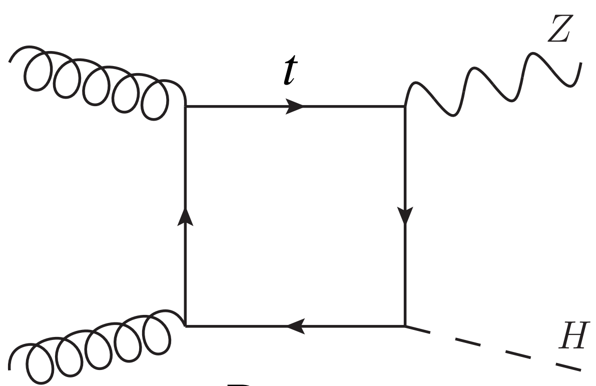

Box

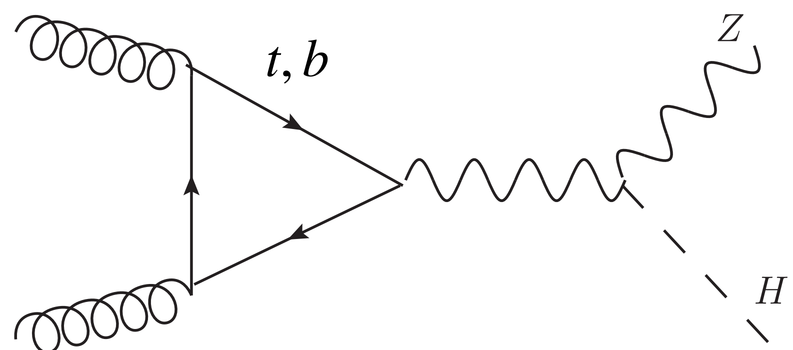

Triangle

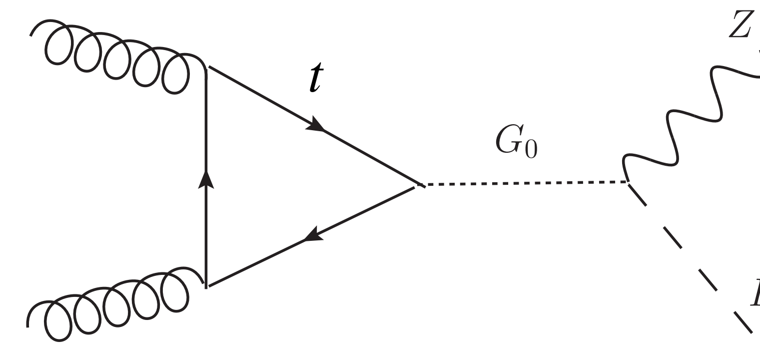

Goldstone

NLO (2-loop) Virtual Diagrams

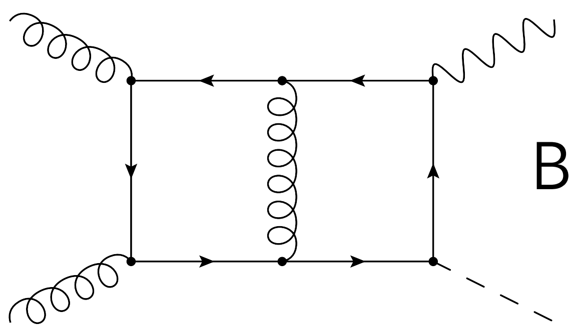

Box

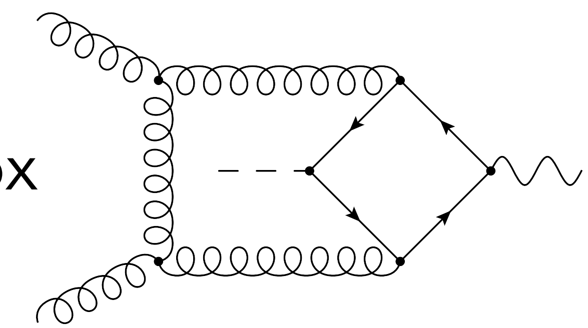

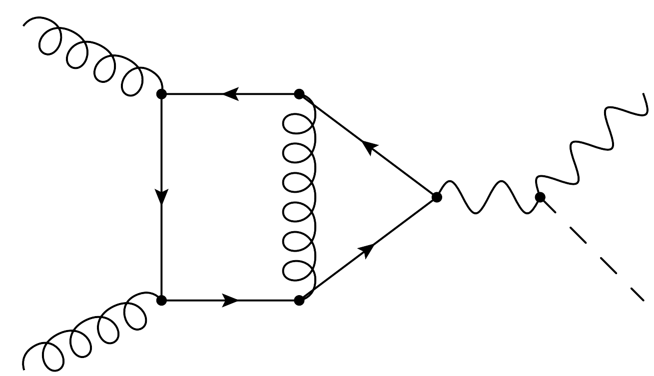

Triangle &
Goldstone

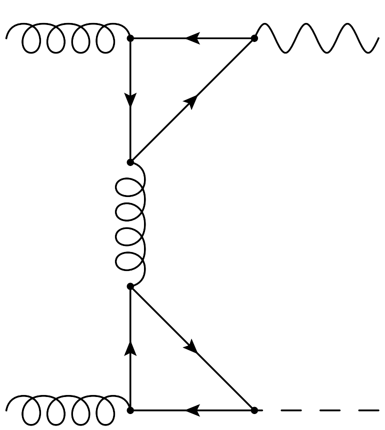

1PR
(start at 2-loop)

We compute in Feynman Gauge

Keep the dependence on all EW couplings symbolic (can be varied)

Set $m_b = 0$

Decomposition: $gg \to ZH$

Idea: construct projectors for linearly polarised amplitudes in c.o.m frame, directly compute polarised amplitudes Chen 19; See also Peraro, Tancredi 19, 20;

Polarisation vectors can be expressed (up to normalisation factors $\mathcal{N}_i$) in terms of external momenta:

$$
\begin{aligned}
\varepsilon_x^\mu =& \mathcal{N}_x \left(-s_{23} p_1^\mu - s_{13} p_2^\mu + s_{12} p_3^\mu\right) \\
\varepsilon_y^\mu =& \mathcal{N}_y \left(\epsilon^\mu_{\mu_1\,\mu_2\,\mu_3}\, p_1^{\mu_1}\, p_2^{\mu_2}\, p_3^{\mu_3}\right) \\
\varepsilon_T^\mu =& \mathcal{N}_T \left(\left(-s_{23}(s_{13}+s_{23}) + 2m_z^2 s_{12}\right) p_1^\mu + \right. \\
& \left. \left(s_{13}(s_{13}+s_{23}) - 2m_z^2 s_{12}\right) p_2^\mu + s_{12}(-s_{13}+s_{23})\, p_3^\mu \right) \\
\varepsilon_l^\mu =& \mathcal{N}_l \left(-2m_z^2 \left(p_1^\mu + p_2^\mu\right) + (s_{13}+s_{23})\, p_3^\mu\right)
\end{aligned}
$$

$$
\begin{aligned}
\varepsilon_x \cdot \{p_1, p_2\} &= 0 \\
\varepsilon_y \cdot \{p_1, p_2\} &= 0 \\
\{\varepsilon_y, \varepsilon_T, \varepsilon_l\} \cdot p_3 &= 0 \\
\varepsilon_i^2 &= -1
\end{aligned}
$$

Projectors are just products of pol. vecs.

$$
\begin{aligned}
\mathcal{P}_1^{\mu_1\mu_2\mu_3} &= \varepsilon_x^{\mu_1}\, \varepsilon_x^{\mu_2}\, \varepsilon_y^{\mu_3} & \mathcal{P}_2^{\mu_1\mu_2\mu_3} &= \varepsilon_x^{\mu_1}\, \varepsilon_y^{\mu_2}\, \varepsilon_T^{\mu_3}, \\
\mathcal{P}_3^{\mu_1\mu_2\mu_3} &= \varepsilon_x^{\mu_1}\, \varepsilon_y^{\mu_2}\, \varepsilon_l^{\mu_3} & \mathcal{P}_4^{\mu_1\mu_2\mu_3} &= \varepsilon_y^{\mu_1}\, \varepsilon_x^{\mu_2}\, \varepsilon_T^{\mu_3}, \\
\mathcal{P}_5^{\mu_1\mu_2\mu_3} &= \varepsilon_y^{\mu_1}\, \varepsilon_x^{\mu_2}\, \varepsilon_l^{\mu_3} & \mathcal{P}_6^{\mu_1\mu_2\mu_3} &= \varepsilon_y^{\mu_1}\, \varepsilon_y^{\mu_2}\, \varepsilon_y^{\mu_3}.
\end{aligned}
$$

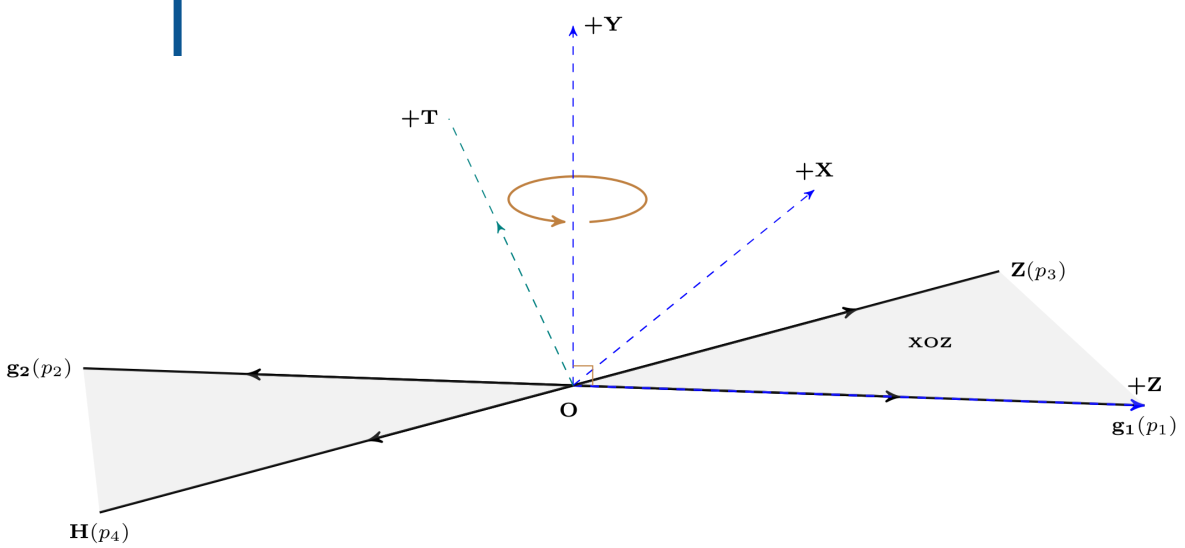

Cross checked with conventional form factor decomposition at LO and at NLO with expansions Davies, Mishima, Steinhauser 20

Dimensional Regularisation & γ_5

Z-Fermion Vertex

Contains vector $\sim v_t \gamma_\mu$ and axial-vector $\sim a_t \gamma_\mu \gamma_5$:

$$\mathscr{V}_\mu^{Vf\bar{f}} = i \frac{e}{2 \sin \theta_W \cos \theta_W} \gamma_\mu \left(v_t + a_t \gamma_5 \right)$$

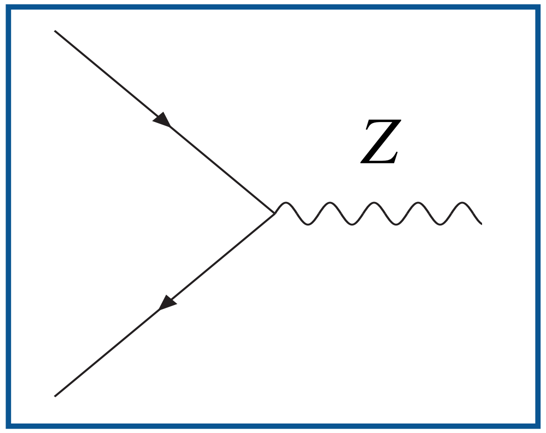

We use dimensional regularisation ($d = 4 - 2\epsilon$) to regulate divergences appearing in loop integrals, however, one can't retain all properties of γ_5 in $d \neq 4$ dimensions

Larin Scheme (Used here)

Sacrifice anti-commuting property of γ_5

$$J_\mu^5 = Z_{5,ns} \; J_{\mu,B}^5 = Z_{5,ns} \; \left[\frac{i}{3\,!} \epsilon_{\mu\nu\rho\sigma} \bar{\psi} \gamma^\nu \gamma^\rho \gamma^\sigma \bar{\psi} \right]$$

$$P^5 = Z_{5,p} \; P_B^5 = Z_{5,p} \; \left[\frac{i}{4\,!} \epsilon_{\mu\nu\rho\sigma} \bar{\psi} \gamma^\mu \gamma^\nu \gamma^\rho \gamma^\sigma \bar{\psi} \right]$$

Fix Ward identities/ABJ anomaly:

$$Z_{5,ns} = 1 + \alpha_s(-4C_F) + \dots$$
$$Z_{5,p} = 1 + \alpha_s(-8C_F) + \dots$$

Larin, Vermaseren 91; Larin 93

Alternative schemes exist e.g:

Kreimer Scheme

Retain $\{\gamma_5, \gamma^\mu\} = 0$, but, sacrifice cyclicity of traces involving γ_5

Define `reading point' and carefully manipulate all traces

Kreimer 90; Korner, Kreimer, Schilcher 92

Amplitudes

Schematically:

$\mathcal{M}^{\mu\nu\rho} \sim$ 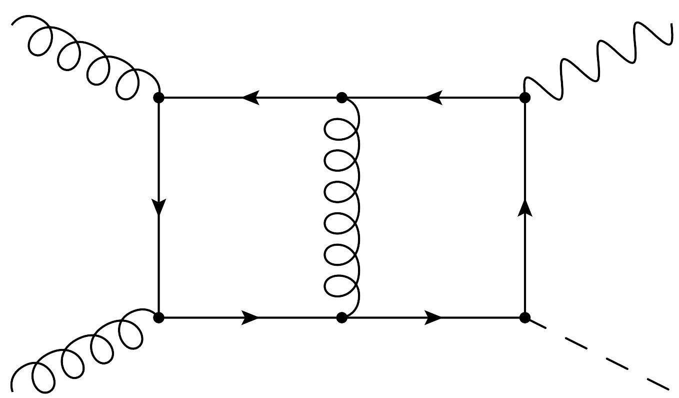 $+$ 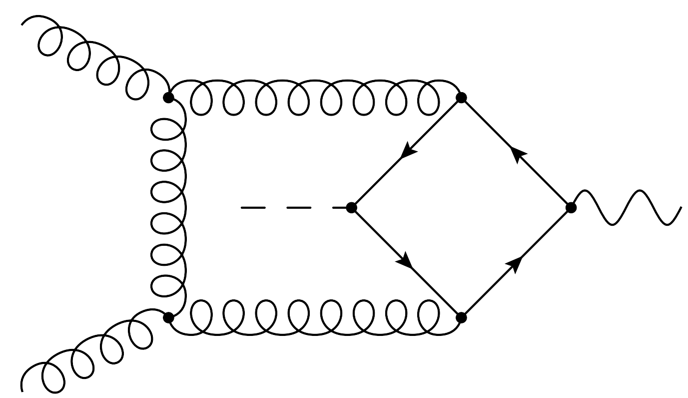 $+ \ldots$

$$\mathcal{M}^{\mu\nu\rho} = \sum_i A_i T_i^{\mu\nu\rho}, \qquad A_i = \sum_k C_{i,k}\ I_k$$

Rational functions
Large num. terms/ high degree
Handled with FORM & FireFly

Vermaseren 00; Kuipers, Ueda, Vermaseren 13; Ruijl, Ueda, Vermaseren 17; Klappert, Lange 19; Klappert, Klein, Lange 20

Feynman integrals
Analytically: Involved special functions (Polylogs, Elliptic…)

In our work, we will compute them numerically or in a small-m_t expansion

Dealing with the Integrals

Integral Reduction

Reduce to master integrals using Kira 2 + FireFly

Mass ratios fixed $\frac{m_z^2}{m_t^2} = \frac{23}{83}, \frac{m_H^2}{m_t^2} = \frac{12}{23}$

Maierhöfer, Usovitsch, Uwer 18;
Klappert, Lange, P. Maierhöfer, Usovitsch 20;
Klappert, Lange 20; Klappert, Klein, Lange 20

Obtain 452 master integrals

Basis:

1) Select quasi-finite integrals
2) Require d- and kinematic dependence of denominators factorises (achieved by brute force neglecting sub-sectors, public tools are available)

Smirnov, Smirnov 20; Usovitsch 20

$$\frac{N(s,t,d)}{D(s,t,d)} I + \ldots \rightarrow \frac{N'(s,t,d)}{D_1'(d) D_2'(s,t)} I' + \ldots$$

3) Prefer simple denominator factors
4) Prefer fewer orders in epsilon for each master (found a basis in which all 7-propagator integrals start contributing only at ϵ^{-1})
5) Prefer simpler numerators (check number of terms/file size)

See: Matthias Kerner, Loops and Legs Proceedings 2018

Steps 2-5 reduced the size of amplitude by factor of 5

Largest coefficient (double-tadpole) 150 MB → 5 MB

Evaluation of the Integrals

Integrals evaluated numerically on GPUs using sector decomposition (**pySecDec**) (written in python, FORM, c++, CUDA)
Vermaseren 00; Kuipers, Ueda, Vermaseren 13; Ruijl, Ueda, Vermaseren 17

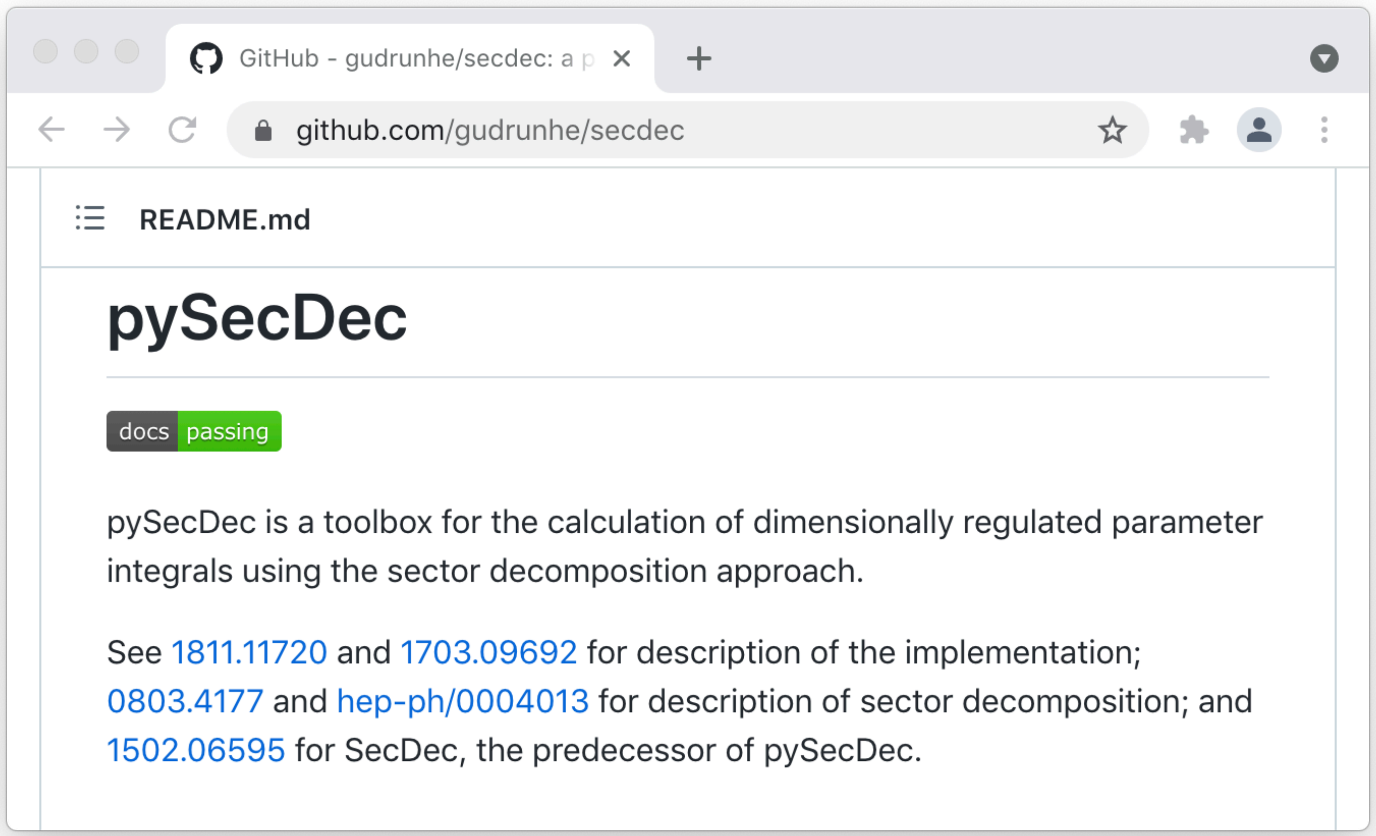

Publicly available (Github)

Extensive tests (CI) and documentation

Install with:

```
python3 -m pip install --user --upgrade pySecDec
```

Latest update: Expansion by Regions & Amplitude Evaluation
Heinrich, Jahn, SPJ, Kerner, Langer, Magerya, Põldaru, Schlenk, Villa 21

→See talk of Vitaly

Combining with expanded results

Comparison to Small m_t Expansion

The amplitude can be expanded around small m_t, m_h, m_z Davies, Mishima, Steinhauser 20; Mishima 18

Previously known to $(m_z^2,\ m_h^2,\ m_t^{32})$, extended for this work to $(m_z^4,\ m_h^4,\ m_t^{32})$

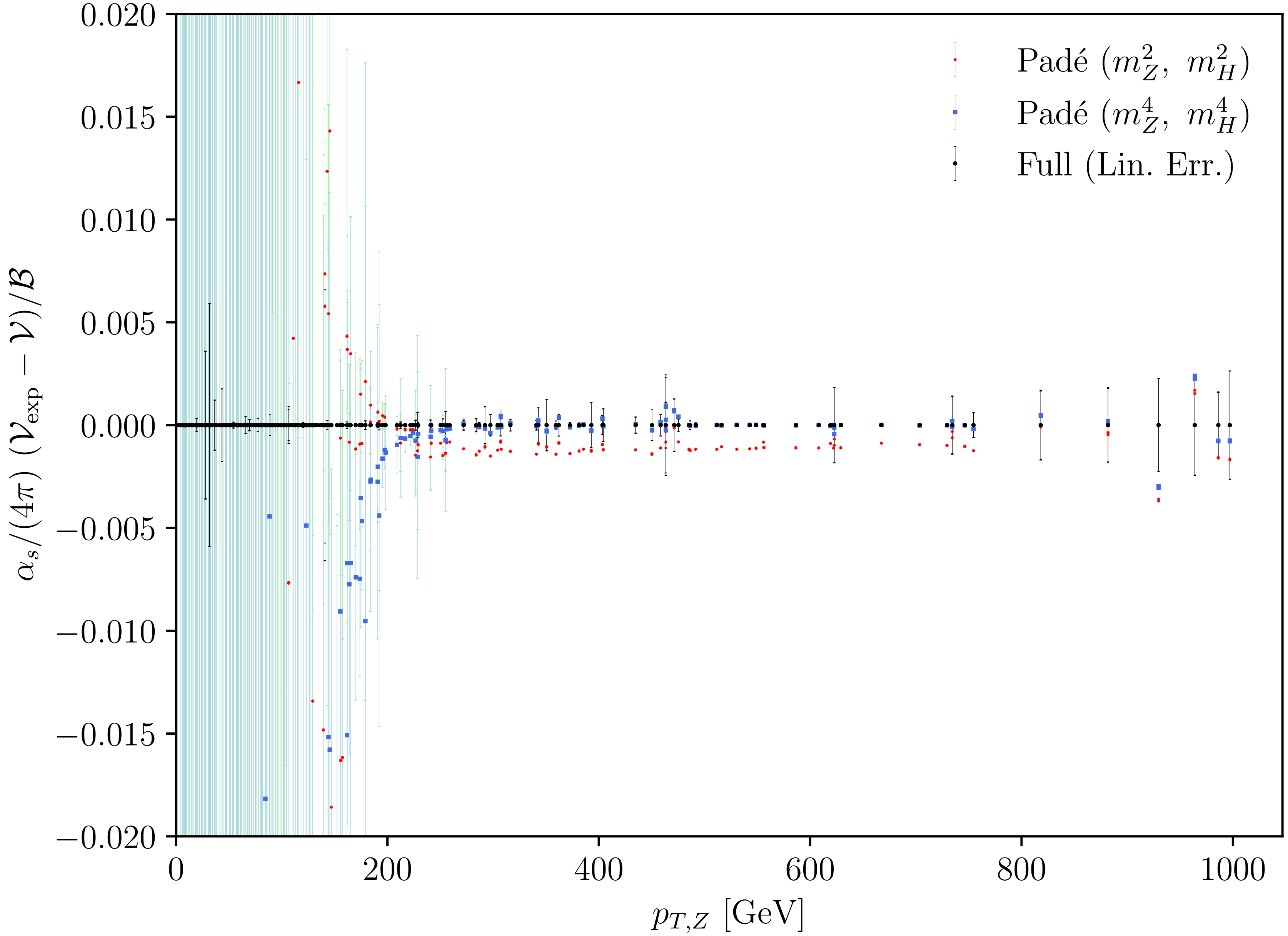

Find **acceptable** agreement for $p_{T,Z} \geq 150$ GeV (<2.8% difference)
Switch from the full numerical result to Padé result at this point

Results $gg \to ZH$

Real Emission Diagrams

There is some **freedom** regarding which real diagrams we include in gg vs $q\bar{q}$

Must be careful not to double count when combining all channels for $pp \to ZH$

Our reals are evaluated using **GoSam** Cullen et al. 11,14

Diagrams included in our work ($n_f = 5$ + massive top in loop) + crossings

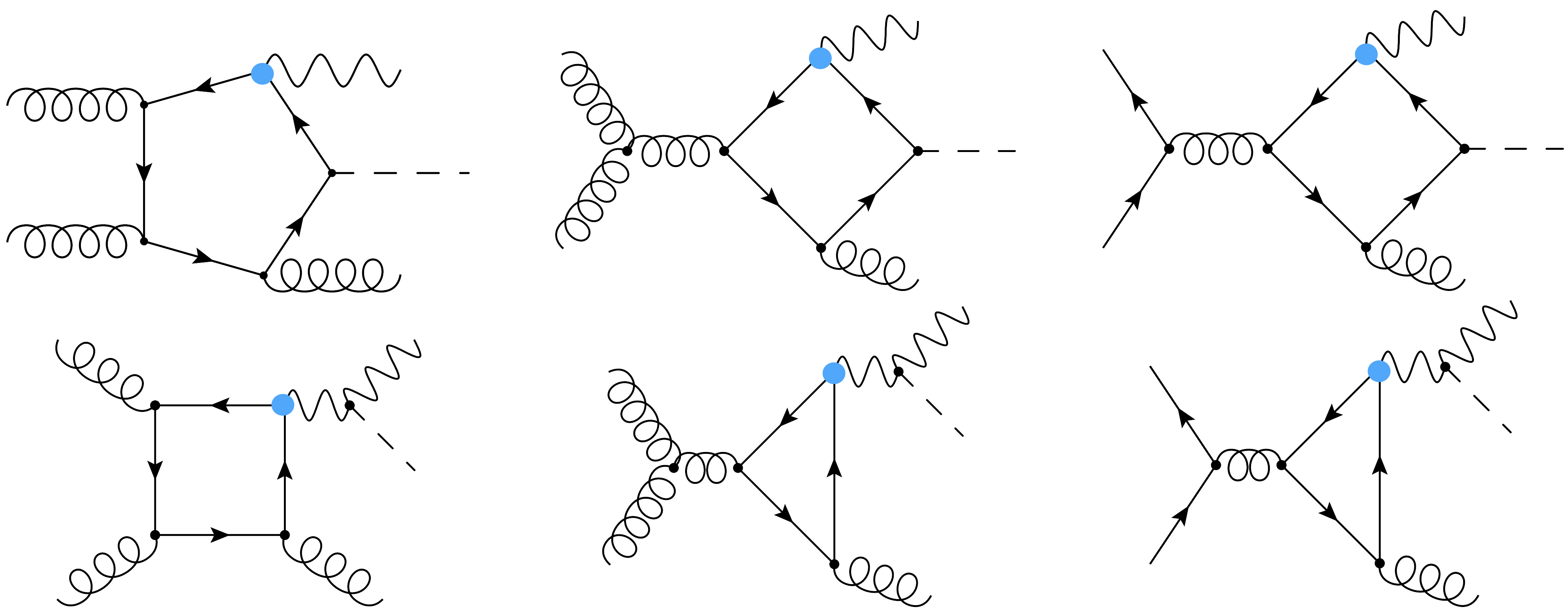

We require:

1) A closed fermion loop
2) A Z-boson or Goldstone boson coupled to that loop

Real Emission Diagrams (II)

There is some **freedom** regarding which real diagrams we include in gg vs $q\bar{q}$

Must be careful not to double count when combining all channels for $pp \to ZH$

Our reals are evaluated using **GoSam** Cullen et al. 11,14

Diagrams excluded in our work

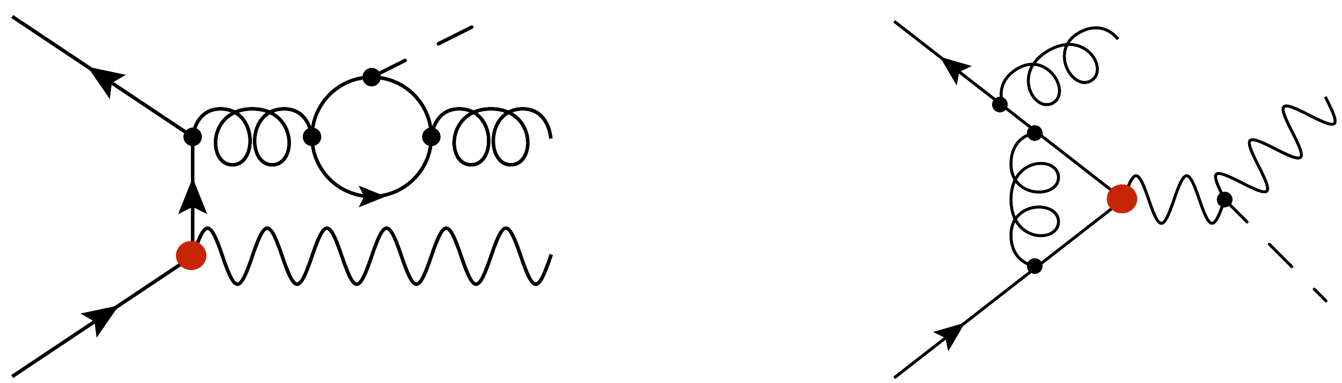

Left class of diagrams: separately UV/IR finite & gauge invariant

Previously studied in detail See e.g. Brein, Harlander, Wiesemann, Zirke 12

Right class of diagrams: belongs to real corrections to Drell-Yan (i.e. $q\bar{q}$)

Included in DY calculations Brein, Djouadi, Harlander 03; Ferrera, Grazzini, Tramontano 14; See also: Kumara, Mandal, Ravindran 14

Total Cross Section & Invariant Mass

Total Cross Section

$\sqrt{s}$	LO [fb]	NLO [fb]
13 TeV	$52.42^{+25.5\%}_{-19.3\%}$	$103.8(3)^{+16.4\%}_{-13.9\%}$
13.6 TeV	$58.06^{+25.1\%}_{-19.0\%}$	$114.7(3)^{+16.2\%}_{-13.7\%}$
14 TeV	$61.96^{+24.9\%}_{-18.9\%}$	$122.2(3)^{+16.1\%}_{-13.6\%}$

NNPDF31_nlo_pdfas

$m_t^{\mathrm{OS}} = 173.21$ GeV

$\mu = m_{ZH}$

$\mu_{R,F} \in \left[\frac{\mu}{2}, 2\mu\right]$ (7 – point)

Invariant Mass

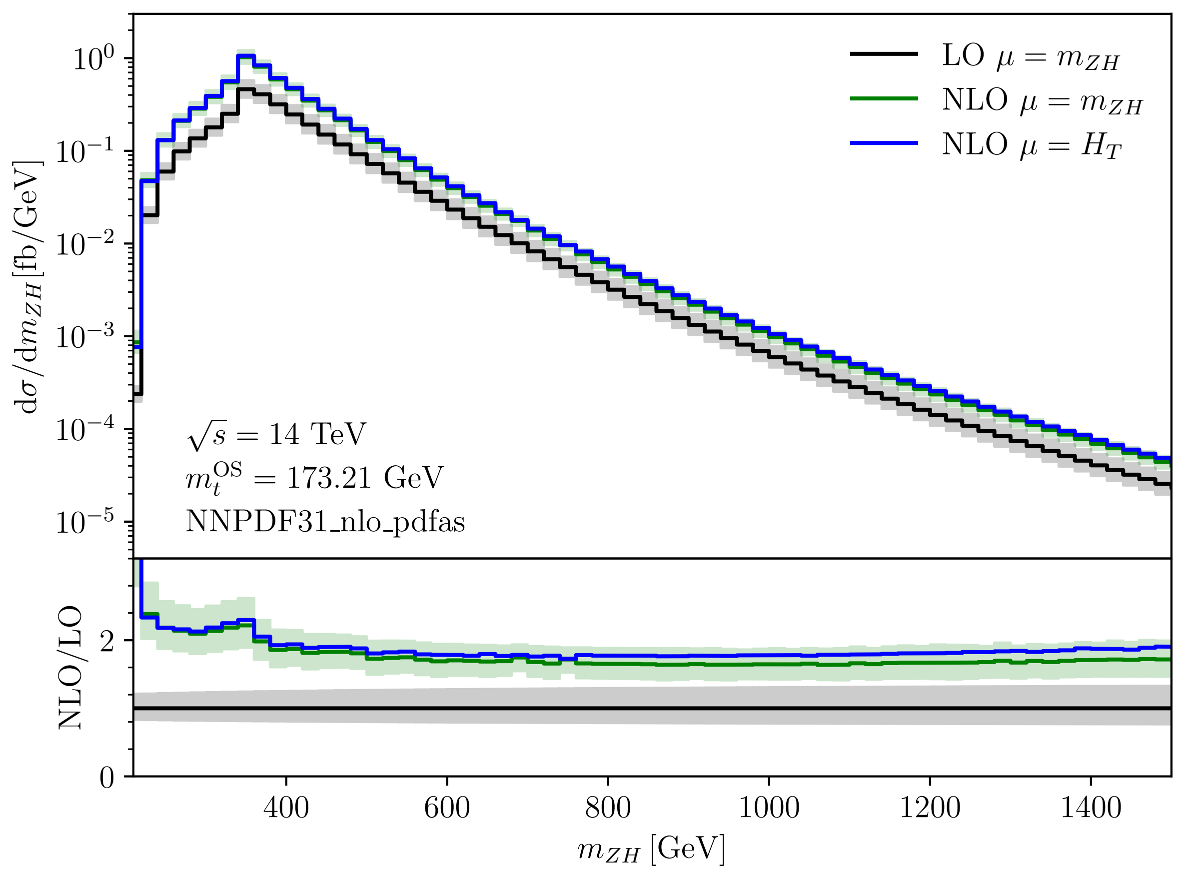

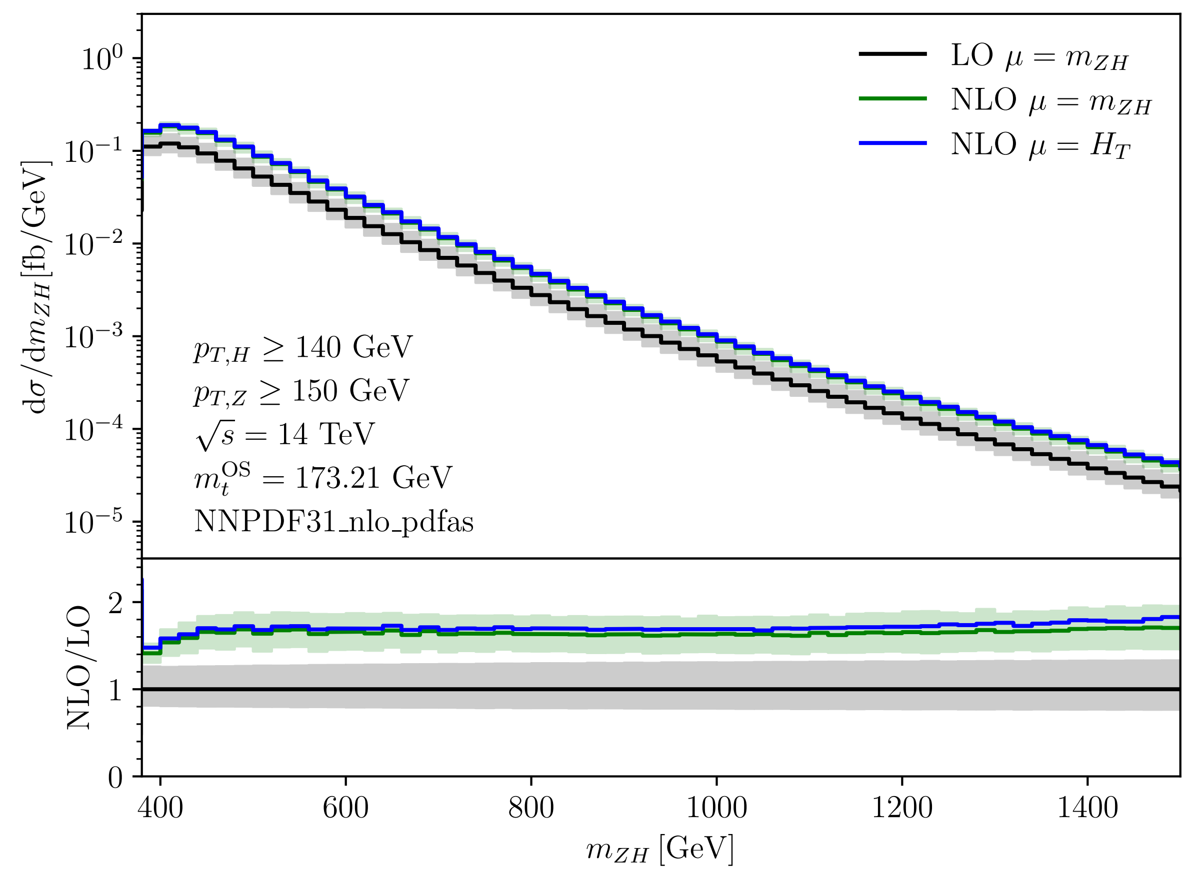

NLO/LO somewhat flat except at production & top pair production thresholds

Comparison to Expansion (Small m_h, m_z)

Can expand in only m_h, m_z and retain full m_t dependence Wang, Xu, Xu, Yang 21

Integrals appearing in the expansion (scales s, t, m_t^2) are known

Caron-Huot, Henn 14; Becchetti, Bonciani 18; Xu, Yang 18; Wang, Wang, Xu, Xu, Yang 20;

Expansion shows good agreement with numerical result

No breakdown near top threshold

$\hat{s}/m_t^2$	$\hat{u}/m_t^2$	$\mathcal{V}'_{\mathrm{fin}}$			
		pySecDec	$\mathcal{O}(m^0)$	$\mathcal{O}(m^2)$	$\mathcal{O}(m^4)$
1.707133657190554	−0.441203767016323	35.429092(6)	35.9823	35.5530	35.4478
3.876056604162662	−1.616287256345735	4339.045(1)	4319.37	4336.63	4338.73
4.130574250302561	−1.750372271104745	6912.361(3)	6870.47	6906.92	6911.64
4.130574250302561	−2.595461551488002	6981.09(2)	6979.28	6980.14	6980.85
134.5142052093564	−70.34125943305149	−153.9(4)	−154.543	−154.458	−154.460
134.5142052093564	−105.1770655376327	527(4)	524.585	525.958	525.965

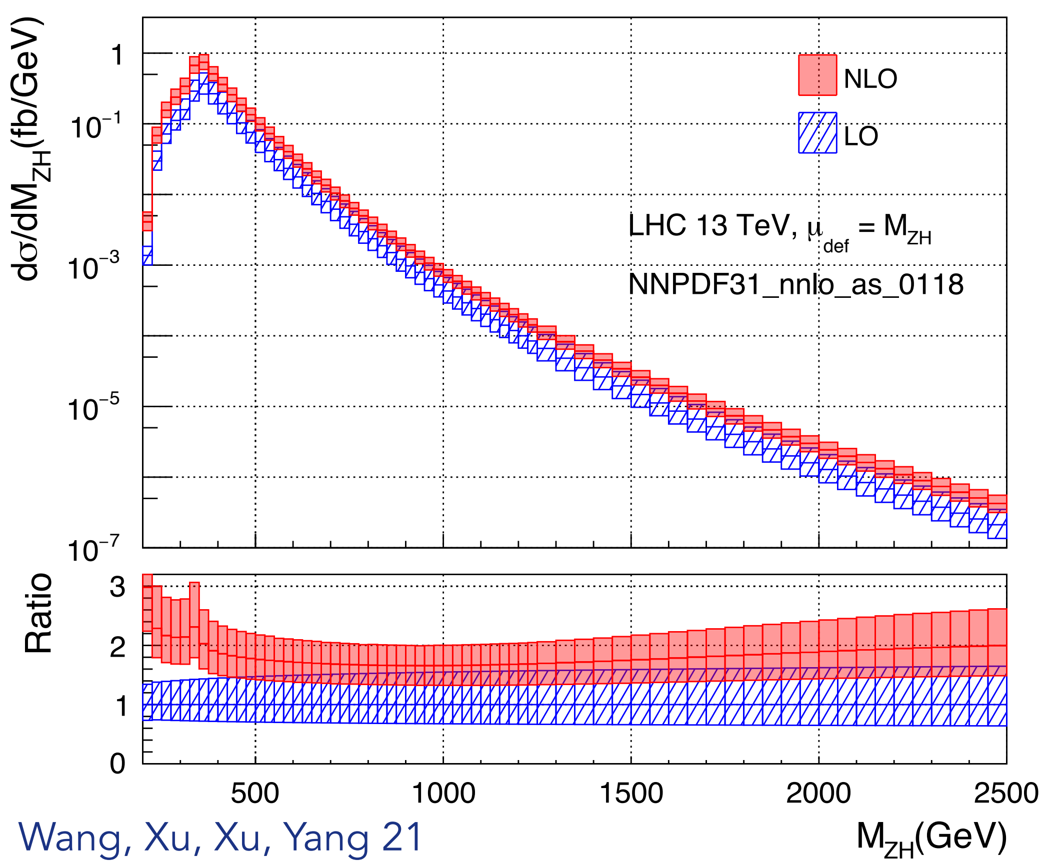

Wang, Xu, Xu, Yang 21

Authors obtained NLO results for $gg \to ZH$

Virtuals: small m_h, m_z expansion

Reals: GoSam Cullen et al. 11, 14

We find agreement with their total cross section result and uncertainty

(2% difference ascribed to different choice of PDFs and masses)

Z Transverse Momentum

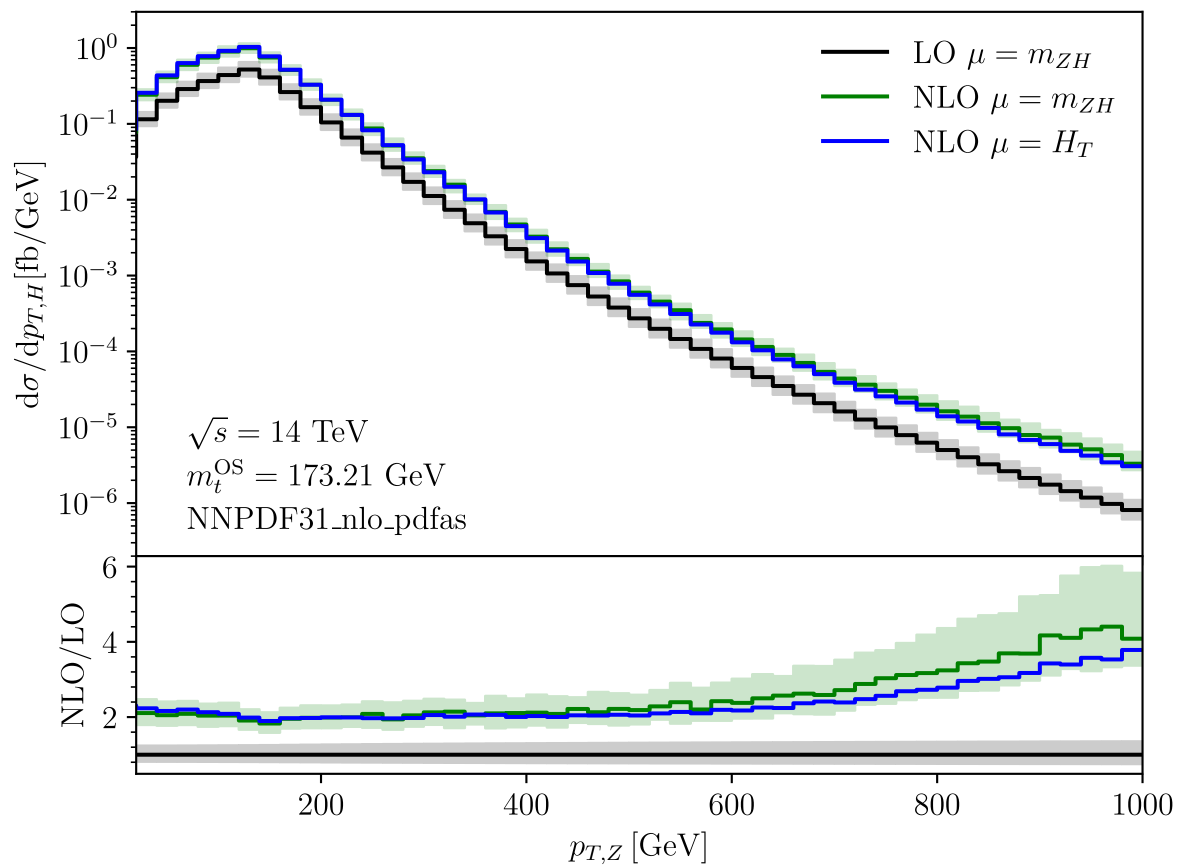

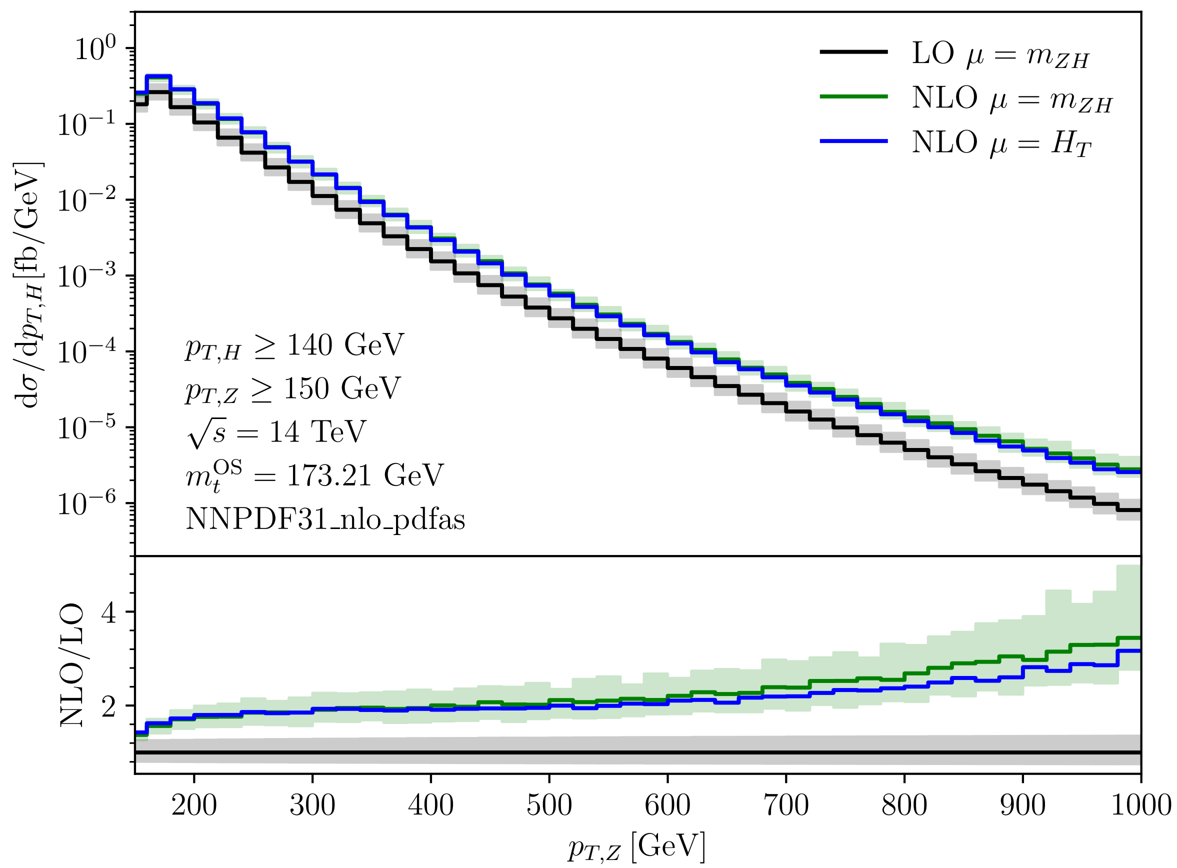

Large NLO corrections, rising sharply at large $p_{T,Z}$

Placing cuts on soft H emission only slightly tames growth

Very important to include higher order corrections in this region

H Transverse Momentum

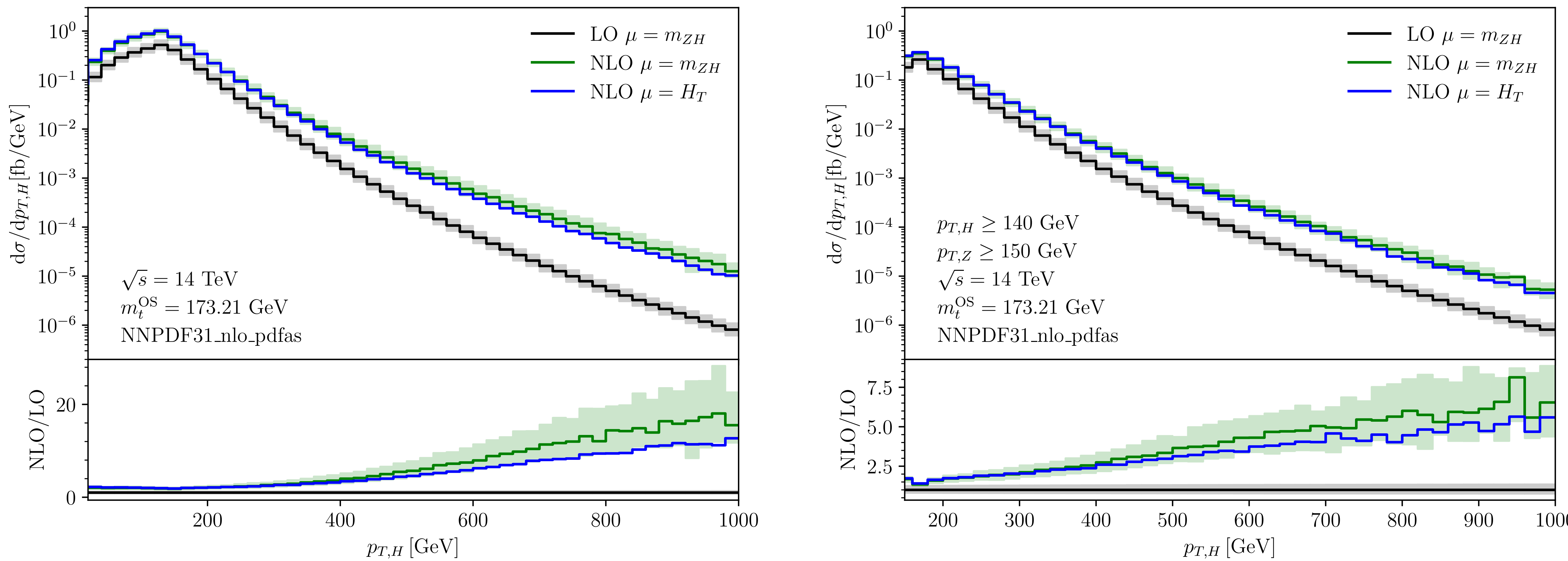

Extremely large pathological NLO corrections, rising very sharply at large $p_{T,H}$
Placing cuts on soft Z emission tames growth somewhat

Let's try to understand what is leading to this different behaviour for $p_{T,Z}$ vs $p_{T,H}$

Discussion: Z vs H

The different behaviour of $p_{T,Z}$ and $p_{T,H}$ was observed previously in $gg \to ZH + j$

Hespel, Maltoni, Vryonidou 15; Les Houches 19

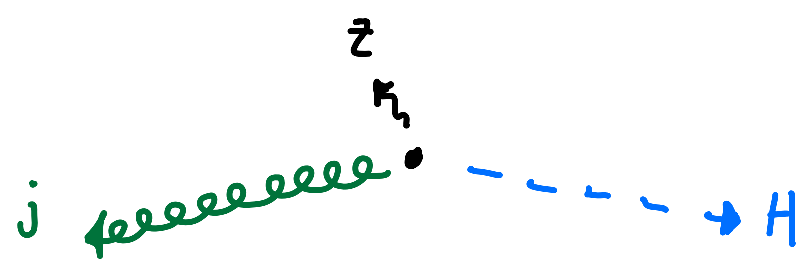

Traced to configurations where Higgs recoils against a hard jet, with a soft Z

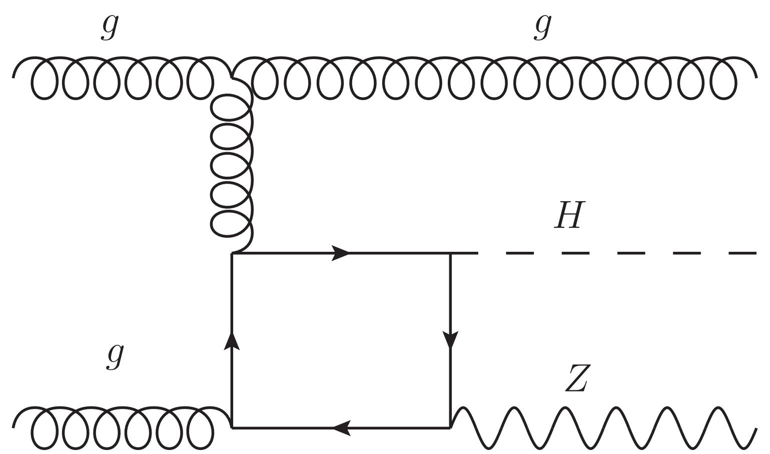

Maltoni et al. attributed this t-channel gluon exchange

One observation

If we apply an eikonal approximation to such diagrams, the enhancement of soft Z bosons can be understood

$$(\text{Soft } Z \text{ emission}) : \frac{p^\mu}{p \cdot p_Z}$$

$$(\text{Soft } H \text{ emission}) : \frac{m_t}{p \cdot p_H}$$

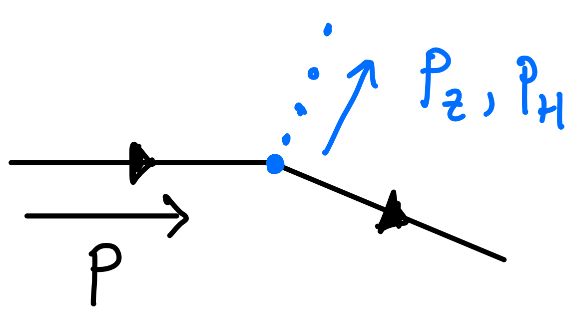

Ratio for large radiator (transverse) momentum $\sim p_T / m_t \gg 1$

Mass Scheme Uncertainty

Can assess impact of changing top quark mass renormalisation scheme for $p_{T,H} \geq 140$ GeV & $p_{T,Z} \geq 150$ GeV using full B + full R + expanded virtuals

HH: Baglio, Campanario, Glaus, Mühllleitner, Spira, Streicher 18 + Ronca 20, 21;
$t\bar{t}$: Catani, Devoto, Grazzini, Kallweit, Mazzitelli 20; $t\bar{t}H$: Martin, Moch, Saibel 21
$t\bar{t}j$: Alioli, Fuster, Garzelli, Gavardi, Irles, Melini, Moch, Uwer, Voß 22; Various: Les Houches 19

Convert $m_t \rightarrow \overline{m}_t(\overline{m}_t)$ using 4-loops, then use RGE at 5-loops with $n_f = 6$
Gives $m_t = 173.21$ GeV $\rightarrow$ $\overline{m}_t(\overline{m}_t) = 163.39$ GeV
Chetyrkin, Kuhn, Steinhauser 00; Herren, Steinhauser 18

Go from OS to $\overline{\text{MS}}$ mass counter term using:

$$m_t \rightarrow \overline{m}_t(\mu_t)\left(1 + \frac{\alpha_s(\mu_R)}{4\pi} C_F \left\{4 + 3\log\left[\frac{\mu_t^2}{\overline{m}_t(\mu_t)^2}\right]\right\}\right)$$

Study 3 different renormalisation scales:

$$\mu_t = m_{ZH},$$
$$\mu_t = H_T = \sum_{i=H,Z}\sqrt{m_i^2 + p_{T,i}^2} + \sum_k |p_{T,k}|$$
$$\mu_t = \overline{m}_t(\overline{m}_t)$$

Mass Scheme Uncertainty

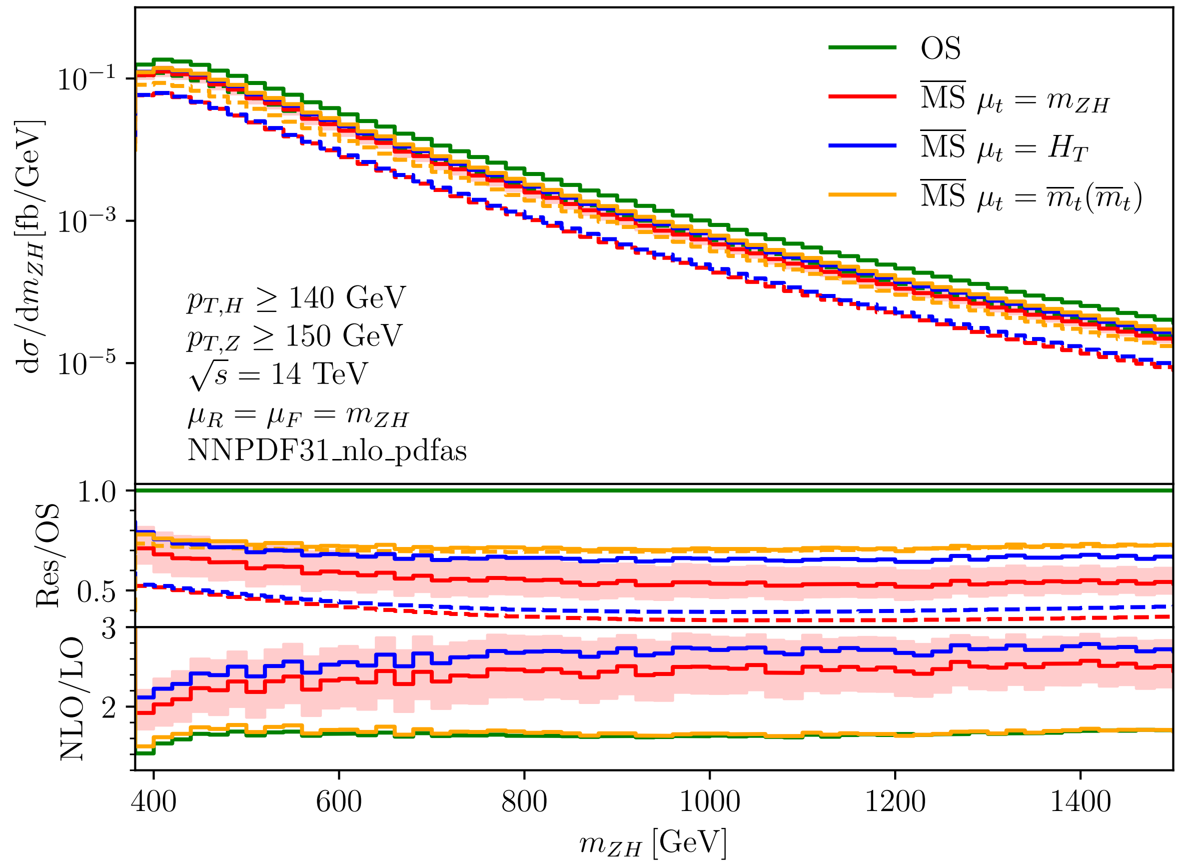

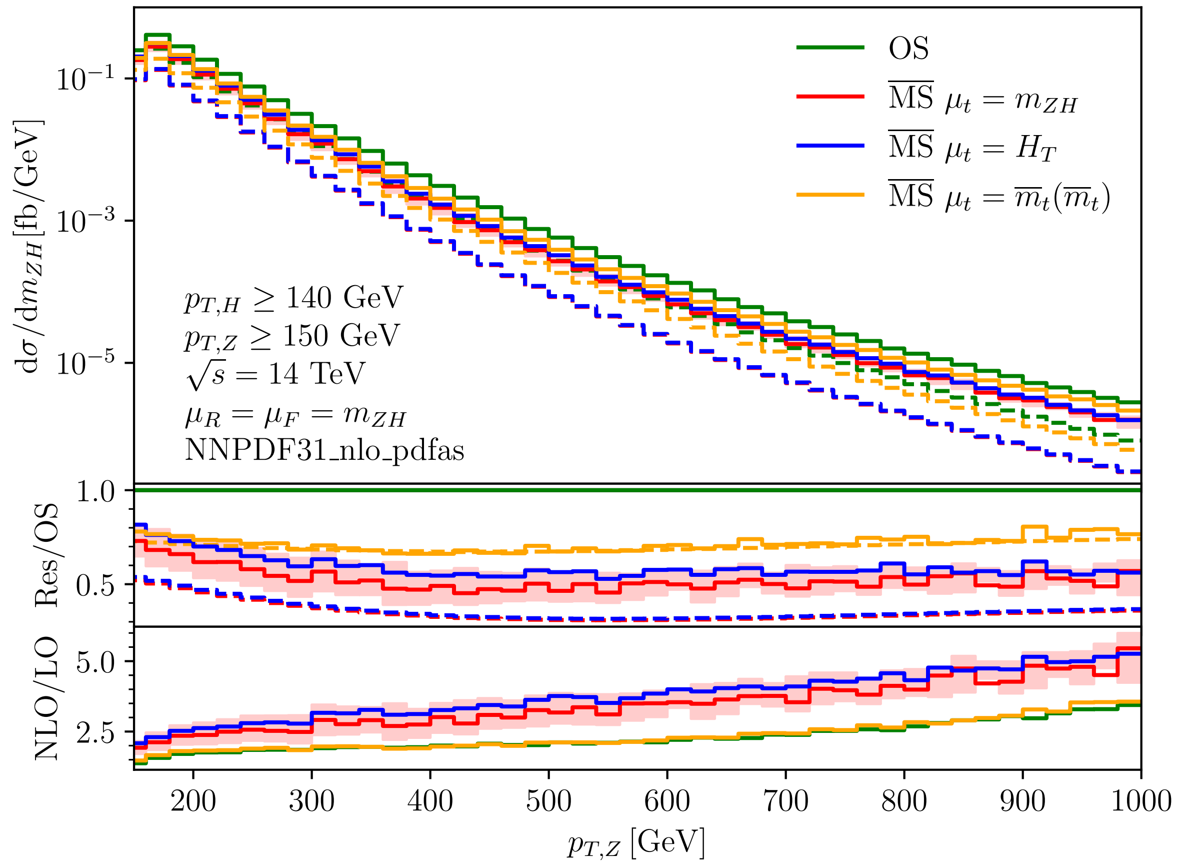

Observations @ $m_{ZH} = 1$ TeV

Large difference between different schemes

- LO: OS result ~2.9x $\overline{\text{MS}}$ result
- NLO: Difference reduced ~1.9x

Scale $\mu_t = \overline{m}_t(\overline{m}_t)$ most similar to OS (OS is 1.4x)

Scale $\mu_t = m_{ZH}$ differs most from OS (OS is 1.9x)

If taken as a theoretical uncertainty, is much larger than scale uncertainty

Mass Scheme Uncertainty

Comparing to $gg \to HH$, we see a different high-energy behaviour

$$A_i^{\text{fin}} = a_s A_i^{(0),\text{fin}} + a_s^2 A_i^{(1),\text{fin}} + \mathcal{O}(a_s^3) \quad \text{with} \;\; a_s = \alpha_s/4\pi$$

HH Davies, Mishima, Steinhauser, Wellmann 18; Baglio, Campanario, Glaus, Mühlleitner, Ronca, Spira, Streicher 20

$$A_i^{(0)} \sim m_t^2 f_i(s,t)$$

$$A_i^{(1)} \sim 6 C_F A_i^{(0)} \log \left[\frac{m_t^2}{s} \right]$$

LO: m_t^2 from y_t^2

NLO: leading $\log(m_t^2)$ from mass c.t.

converting to $\overline{\text{MS}}$ gives $\log\left[\mu_t^2/s\right]$

motivating scale choice of $\mu_t^2 \sim s$

ZH Davies, Mishima, Steinhauser 20

$$A_i^{(0)} \sim m_t^2 f_i(s,t) \;\; \log^2 \left[\frac{m_t^2}{s} \right]$$

$$A_i^{(1)} \sim \frac{(C_A - C_F)}{6} A_i^{(0)} \;\; \log^2 \left[\frac{m_t^2}{s} \right]$$

LO: one m_t from y_t

NLO: leading $\log(m_t^2)$ not coming from mass c.t. (C_A)

Would be interesting to further understand these structures, similar power-suppressed mass logarithms were studied in single H Liu, Modi, Penin 22

Conclusion

I have presented a calculation which underscores the usefulness of

- Numerical methods for solving Feynman integrals
- Using expansions, where valid, to supplement numerical results and explore the analytic structure

Next steps…

- Incorporate into public tools for $pp \to ZH$ (?)

Thank you for listening!

Backup

Comparison to Large m_t Expansion

The amplitude has been expanded around large-m_t and computed analytically
Hasselhuhn, Luthe, Steinhauser 17; Davies, Mishima, Steinhauser 20

Let us compare our result to the Born reweighted $1/m_t^{2n}$ expansion:

$$\mathcal{V}_n = \frac{\mathcal{B}}{\mathcal{B}_n}\widetilde{\mathcal{V}}_n + \mathcal{V}^{1\mathrm{PR}}$$

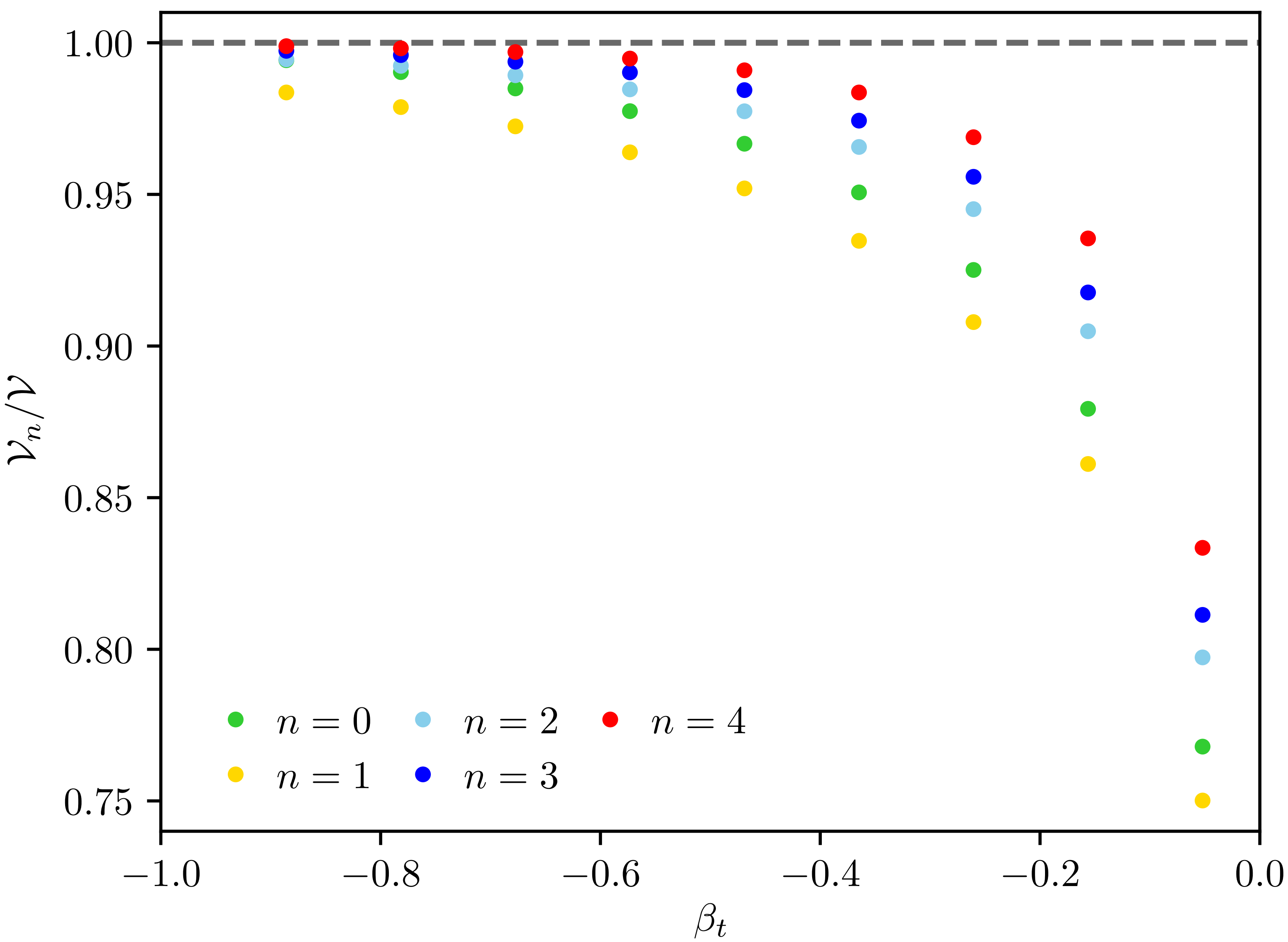

Per mille level agreement far below top quark threshold:

$$\mathscr{V}_4/\mathscr{V} = 0.9989$$

Expansion breaks down at threshold, observe that it differs from our result

Observation: $n = 1$ apparently worse than $n = 0$

Helicity Amplitudes

We can produce precise results for all helicity amplitudes also in kinematic limits!

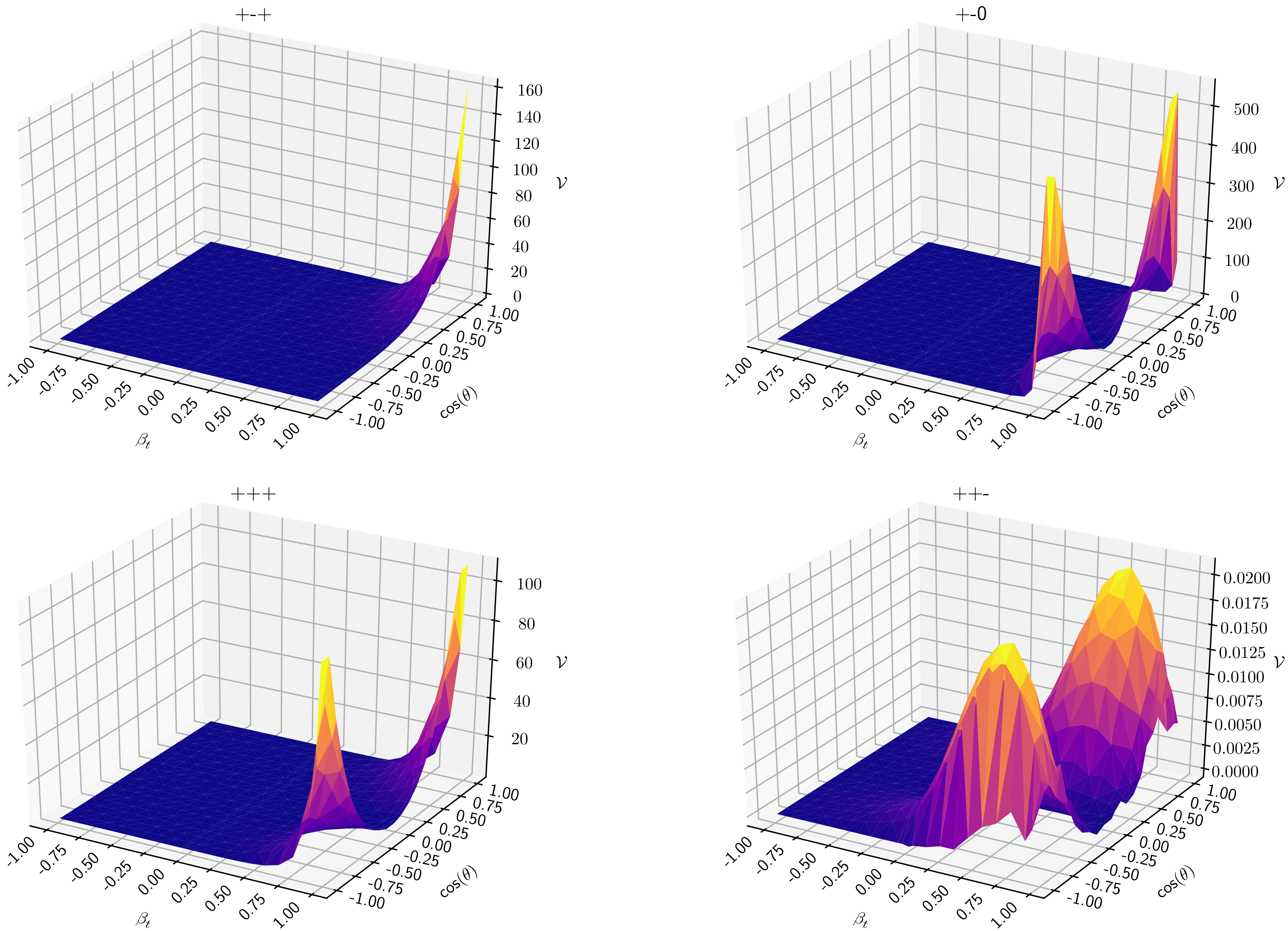

Evaluation of the Amplitude (Timing)

Each phase-space point evaluated with 2 x Nvidia Tesla V100 GPUs
Precision goal set to 0.3% for each (linearly polarised) amplitude

Timing/ point:

Min: 45 mins, **Max:** 24 hr (wall-clock), ~65 hr (high-energy), **Median:** 3.5 hr

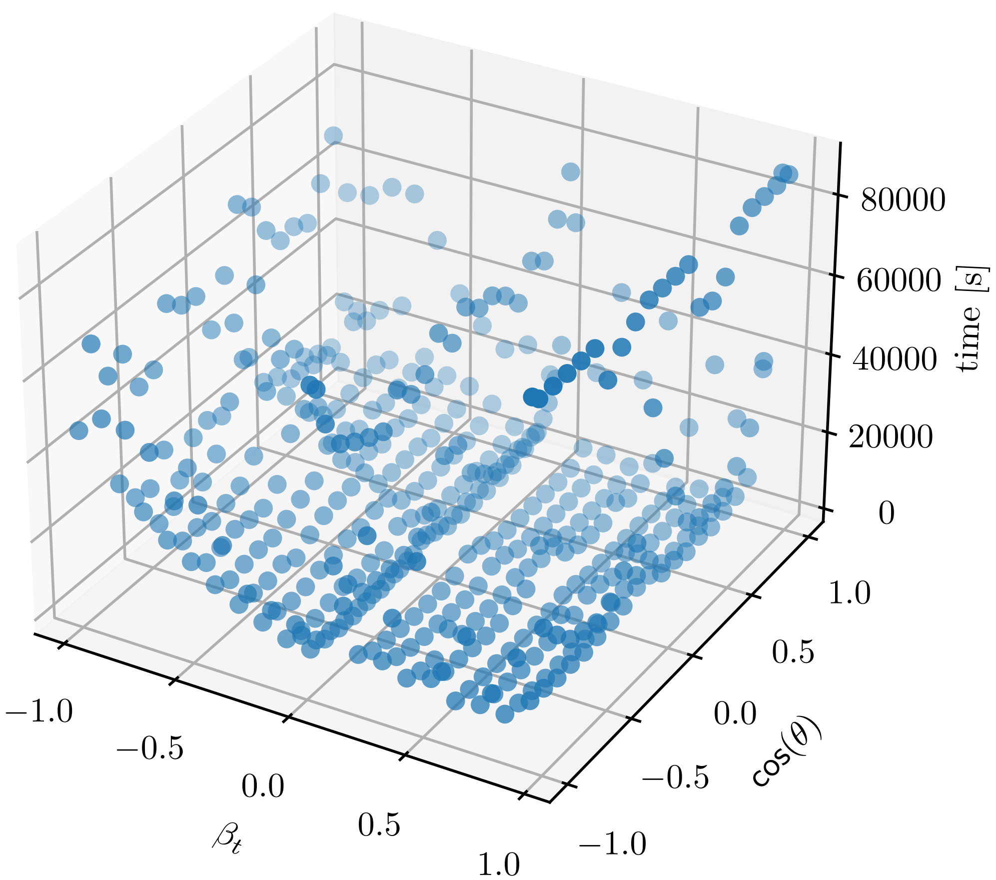

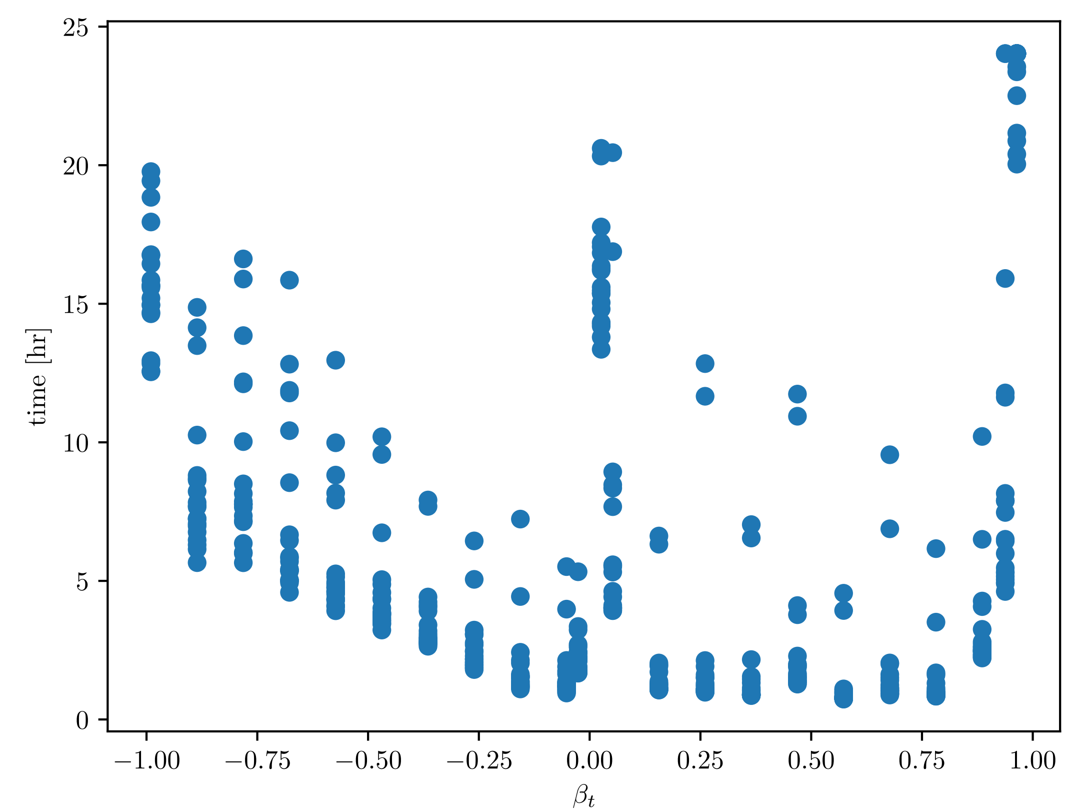

Worst performance near to ZH, $t\bar{t}$ thresholds, high-energy and forward scattering